

Automated extraction of grain-size data from gravel surfaces using digital image processing

Acquisition automatique des données de granulométrie des surfaces de gravier par un procédé d'imagerie numérique

JUSTIN B. BUTLER, Graduate student, Department of Geography, University of Cambridge, Downing Place, CAMBRIDGE, CB2 3EN, U.K.

STUART N. LANE*, Professor, School of Geography, University of Leeds, LEEDS, LS2 9JT, U.K. Email: s.lane@geog.leeds.ac.uk

JIM H. CHANDLER, Senior Lecturer, Department of Civil Engineering, Loughborough University, LOUGHBOROUGH, LE 11 3TU.

ABSTRACT

This paper describes and tests a method for the automated extraction of grain-size data from digital imagery. It combines two basic image processing methods for this purpose: grey-scale thresholding to create a binary image and watershed segmentation to grow edges on the binary image to allow the identification of individual grains. The method is subject to rigorous testing in terms of edge detection and automatic measurement of grain-size information from the edge images, and is also compared with the results obtained from simple direct clast sampling. The edge detection methods are tested with respect to manually-identified edges. This suggests that simple thresholding of raw imagery produces grain-size estimates that are: (i) in excellent agreement with manual estimates, above a critical particle size defined by the scale of the photography; (ii) downgraded with the inclusion of additional edge information from analysis of high resolution digital elevation models (DEMs); and (iii) not affected by the use of raw imagery as opposed to imagery that has been rectified to deal with geometric, tilt and relief distortion effects. The automated ellipse-based measurement method is shown to produce a good estimate of two-dimensional *a*- and *b*- axes as they appear as long and short axes on the edge images. Thus, the research shows that it can be used to map and quantify very rapidly spatial variations in grain-size characteristics, although it cannot deal with the long-recognised problem of the relationship between two-dimensional planform grain-size estimates and actual *a*- and *b*- axes obtained by direct grain sampling.

KEY WORDS

grain size analysis, gravel-bed rivers, hydraulics, image processing, photogrammetry

RÉSUMÉ

Cet article décrit et expérimente une méthode d'acquisition automatique de données granulométriques à partir d'images numériques. Pour ce faire il y a combinaison de deux méthodes de base du traitement d'image : fixation d'un seuil de niveaux de gris pour créer une image binaire, et segmentation par lignes de partage pour accentuer les contours dans l'image binaire afin d'identifier les grains individuellement. La méthode est soumise à des tests rigoureux en termes de détection de bords et de mesure automatique des tailles de grains à partir des images des bords, avec comparaison des résultats obtenus en échantillonnant directement les clastes. Les méthodes de détection de bords sont testées par rapport aux bords identifiés manuellement. Il apparaît que la simple détection de seuil de l'imagerie brute fournit des estimations de granulométrie qui sont : (i) en très bon accord avec les estimations manuelles au-dessus d'une taille critique de particules définie par l'échelle de la photographie ; (ii) affinées par l'introduction d'une information de bord additionnelle donnée par l'analyse des modèles digitaux en élévation (DEMs) de haute résolution ; et (iii) non affectées par l'emploi de l'imagerie brute comparée à l'imagerie qui a été retraitée pour tenir compte des effets de distorsion géométrique dus au relief et aux inclinaisons. Il s'avère que la méthode de mesure automatisée basée sur l'ellipse fournit une bonne estimation des axes bidimensionnels *a*- et *b*- qui apparaissent en tant que petit et grand axe sur les images des bords. Ainsi, l'étude montre que la méthode peut être utilisée pour cartographier et quantifier très rapidement les variations spatiales des caractéristiques granulométriques, cependant elle ne peut pas gérer le problème bien connu de la relation entre les estimations des tailles de grains en représentation bidimensionnelle plane et les axes réels *a*- et *b*- obtenus par l'échantillonnage direct des grains.

MOTS-CLÉS

analyse granulométrique, rivières à lit de gravier, hydraulique, traitement d'image, photogrammétrie.

1. Introduction

Quantification of the grain size distributions of sedimentary deposits remains an issue of immense importance for river channel hydraulics studies in gravel-bed rivers, where surface grain-size characteristics have been central to the estimation of flow resistance (e.g. Strickler, 1923) and sediment transport (e.g. Shields, 1936; Parker *et al.*, 1982; Andrews, 1983; Komar and Li, 1988; Kirchner *et al.*, 1990; Buffington *et al.*, 1992) for considerable time. However, this is not a straightforward task as: (i) there may be marked vertical, lateral and longitudinal variations in bed ma-

terial composition (Kellerhals and Bray, 1971) and attention must be given to ensuring that estimates are based upon a representative sample (for instance, surface and subsurface grains should be sampled separately (e.g. Klingemann and Emmett, 1982), particularly if surface roughness is of interest (e.g. Church *et al.*, 1987)); (ii) the wide particle size-distributions of gravel-bed rivers mean that close attention must be paid to the minimum acceptable sample size required to represent a population accurately and precisely (Iriondo, 1972; Hey and Thorne, 1983; Mosley and Tindale, 1985; Church *et al.*, 1987; Rice and Church, 1996; Ferguson and Paola, 1997); (iii) sediment transport leads to sig-

Revision received June 27, 2000. Open for discussion till February 28, 2002.

nificant temporal variation in the spatial distribution of sediments (e.g. Fahnstock, 1963; Kellerhals, 1967; Church, 1970); and (iv) measurements that require removal of one or more surface clasts (even if they are replaced) will be destructive which, if undertaken in subaqueous zones, may result in inaccuracies as finer material is washed from the sample before it is removed from the water (Pickup, 1981).

These limitations mean that obtaining reliable, spatially-distributed grain size information from both submerged and exposed zones will be time-consuming and hence expensive. Any methods that can be used to increase the ease and speed with which information can be obtained will be of real importance. Photographic approaches (e.g. Iriondo, 1972; Adams, 1979) may offer one alternative, as the images can be acquired rapidly so reducing the amount of time that must be spent in the field. However, they still require time to be spent in the laboratory extracting necessary information. This paper aims to develop the potential of a photographic approach by developing automated methods for extracting grain-size information from digital imagery, whether scanned from photographic film or acquired using digital cameras.

2. Issues in using photographic approaches to grain-size determination

The manual methods of Iriondo (1972) and Adams (1979) were shown to provide reliable grain-size estimates, provided, and following conventional Wolman (1954) sampling, the fraction finer than 8mm was not considered (e.g. Kellerhals and Bray, 1971). The main area for development of the photographic approach is in terms of automating information extraction from the photograph, based upon the principle that grain boundaries are well-defined with respect to the rest of the image (McEwan *et al.*, in press). McEwan *et al.* developed a successful methodology for extracting data from a high resolution DEM, based upon particle edge detection and image segmentation to convert edges into closed regions (particles). Application to test cases, of known grain-size distributions, produced encouraging results.

Use of these photographic approaches requires a number of assumptions. First, it assumes that derived grain size distributions are not affected by either image, relief or tilt distortion. Image distortion results primarily from an optically imperfect lens. If a traditional film-based camera is used, it may also result from imperfect film flatness due to air in the camera back, stretching during image acquisition or processing and scanning. These sorts of effects have been dealt with extensively and for some time by photogrammetrists (e.g. Wolf, 1983) for whom such distortions can significantly affect the quality of the results obtained. However, little is known about the extent to which distortions might affect the results obtained from image analysis for the purpose of grain-size characterisation. Relief distortion refers to the lateral displacements of the image of a point on a photograph due to variation of elevation on the ground. If the camera optical axis is near orthogonal to the surface of interest, and the relative relief of the surface is small, relief and tilt distortion may be small. Research is required to assess the extent to which image, relief and tilt distortion affects grain size parameters that are derived auto-

matically.

Second, automated approaches developed to date (e.g. McEwan *et al.*, in press) have determined grain-size information from high resolution digital elevation models (DEMs) obtained using a precision laser altimeter. Although both laser altimetry and digital photogrammetry (e.g. Butler *et al.*, 1998; Lane *et al.* in press) might provide such information, these techniques may be expensive or difficult to use in the field. An important issue emerges over the extent to which radiometric imagery, in which texture information takes the form of differences in colour or shadow between particles, may be used. McEwan *et al.* (in press) described basic problems in using radiometric imagery rather than DEMs, due to tonal imperfections on the surface of grains, but noted that this was an issue that needed further assessment.

Third, it is recognised that the grain-size estimates derived from photographs will differ from those obtained using grid-by-number counts (e.g. Wolman, 1954) or surface sieving. Evidence suggests that photographically-derived grain-sizes correspond to those obtained from *b*-axis measurements using callipers or square mesh sieving, as long as the smaller visible axis is used. However, grain interactions, imbrication and shadowing effects have shown that photographically-derived median *b*-axes are shorter than those estimated using other methods (Adams, 1979) and that some form of empirical correction may be required. This was possible because: (i) sieve and photographic measures of the standard deviation of particle size were essentially equivalent; (ii) sieve percentiles are biased relative to photographically-estimated percentiles to the same degree that the mean size is biased; and (iii) sieve size frequency distribution curves are similar in shape to distributions from photographs, but are displaced by the bias. Whilst Adams was able to suggest basic correction factors, the magnitude of the required correction will depend upon the magnitude and angle of imbrication (Church *et al.*, 1987) and hence will be specific to the deposit being studied.

Thus, the objectives of this paper are to: (a) develop a methodology for deriving grain-size parameters from radiometric imagery; (b) assess the extent to which such imagery is suitable for this purpose in the absence of high resolution three-dimensional DEMs; and (c) explore the affects of relief and image distortion upon such parameters.

3. Methodology

Given the above objectives, the methodology sought to: (i) produce datasets for analysis that comprised vertical imagery, high resolution DEMs and vertical imagery corrected for the effects of image, tilt and relief distortion (known as orthoimagery); (ii) develop an analytical approach for the extraction of grain-size parameters based upon analysis of vertical imagery and orthoimagery; and (iii) test the approach developed under (ii) using independently acquired data.

3.1 Imagery, high resolution DEMs and image correction

DEMs and corrected imagery were obtained using close range digital photogrammetry. The methods used to obtain and check

the associated results are described in full in Butler *et al.* (1998). In summary, raw imagery was obtained of: (i) water-worked gravels in a laboratory flume; and (ii) exposed gravels on a point bar in the river Affric, Scotland. Field data collection involved gantry-mounted, vertical photography, obtained using semi-metric, dimensionally-stable Hasselblad cameras, and scanned using a photogrammetric scanner at 20 μ m. The camera ‘flying height’ was 2.2m, resulting in 1:24 scale imagery and image pixel dimensions being equivalent to 0.0006 m of gravel surface. This allowed DEMs to be generated using automated photogrammetry at a spacing of 0.003 m. Once the DEMs were generated, these were used to orthorectify the raw imagery to account for the effects of image, tilt and relief distortion (Butler *et al.*, 1998). In the laboratory case, the flume comprised a 0.3 m wide by 8.0 m long test area. Three DEMs were acquired each covering the full flume width and, after stitching together, a total of *ca.* 1 m of the flume’s length. The camera ‘flying height’ was 1.2 m, resulting in 1:13 scale imagery and image pixel dimensions equivalent to 0.00026 m of gravel surface, allowing generation of DEMs at a spacing of 0.0015 m. Both the field and flume DEMs have been subject to intensive data quality tests, in terms of point precision and accuracy and surface precision and accuracy (e.g. Butler *et al.*, 1998; Butler, 1999).

3.2 Extraction of grain-size parameters

Figures 1A through 1C illustrate the three options explored for the extraction of grain-size parameters. Figure 1A involves grain delimitation *without* explicitly using high resolution DEMs to delimit grains, but using imagery that has been properly corrected for image and relief distortion using such topographic information (orthoimagery). Figure 1B combines orthoimagery with addi-

tional edge information extracted from high resolution DEMs. Thus, comparison of the results from 1A and 1B, with respect to independently acquired estimates, allows assessment of the extent to which high resolution DEMs need to be incorporated into the extraction process. Figure 1C is identical to 1A, but uses uncorrected, raw imagery for the data extraction process, and comparison of the results from 1A and 1C helps determine if high resolution topographic information is needed for image rectification prior to grain-size extraction.

Common to each of the methods in Figure 1 is a set of image processing techniques, shown in *italic*. These are concerned with: (i) identification of edges (Figures 1A, 1B and 1C); (ii) combining edge information where more than one source of edge is used (the Boolean OR step in Figure 1B); and (iii) image segmentation, in which detected edges are ‘grown’ to form closed particle boundaries. All of these image processing techniques are standard to image processing packages, and are described briefly. Edge detection uses local pixel variation to identify boundaries between particles (Pal and Pal, 1993), and this may be sequential or parallel (see Davis, 1975). Parallel edge detectors are less computationally demanding and more commonly available, and thus are used for this research. With the use of rectified or unrectified photography, edge detection must be based upon steps in radiometric or brightness properties, which may sometimes be spread over several pixels (Russ, 1995). Extensive testing suggested that the best results were obtained by using a simple threshold to produce a binary image. Automated thresholding methods, based upon properties of the image histogram (e.g. entropy-maximisation, factorisation, moments), tended to produce results which were consistently too high, classifying features that actually belonged to stones as background. Thus, it was decided to threshold subjectively, but to assess the feasibility of this by assessing the effects

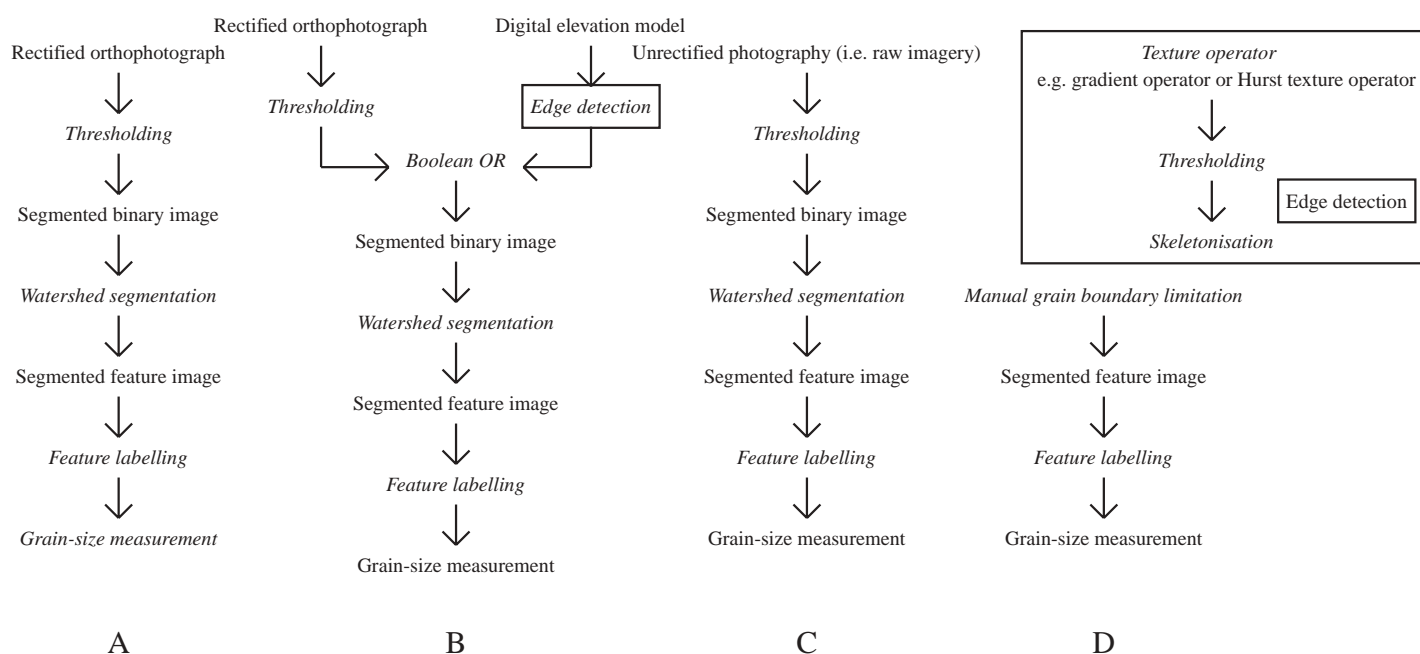


Fig. 1. Summary of method used to generate estimates of grain-size distributions. Processing steps are shown in *italic*. Method A represents the basic approach developed for this research. Method B was introduced to assess if a high resolution DEM was necessary as compared with A. Method C was introduced to assess if rectified orthophotography was necessary as compared with A. Method D was used as a means of assessing the edge detection process in each of A, B and C (i.e. the stages that lead to production of a segmented feature image).

of different threshold values upon grain-size parameters derived from the analysis. From the resultant binary image, the identification of edges was possible through the use of watershed segmentation as an edge interpolation tool (see below).

For the detection of additional edges using topographic data, a different approach was required, with elevations (rather than radiometric properties) between adjacent pixels being used to identify edges. This was based upon a Hurst texture operator (Hurst *et al.*, 1965). At each pixel, the elevation range for a given lag is determined and scaled by the standard deviation of the range for all pixels at that lag: the re-scaled range. This is repeated for all lags and for all pixels. At each pixel, the log of re-scaled range is plotted against the log of lag, and the slope of the best-fit line gives the Hurst dimension, H . This can be calculated reliably from relatively small datasets (Russ, 1994), such that it can readily be applied locally. Areas in a DEM which experience rapid changes in elevation over small distances (i.e. edges) would have high values, such that the H map corresponds to an edge map. The key advantage of the Hurst operator over other gradient operators is that changing the scale (i.e. the number of lags, or pixels) over which H is calculated merely improves the precision of the linear fit to the plot: it is scale independent (Russ, 1994). Once an image of H has been produced, it is necessary to threshold to produce a binary image comprising edges and background, and to skeletonise or thin these edges so that they were a single pixel thick. In practice, the Hurst texture profiler was the best means for detecting edges using the DEMs available for this research, primarily because it was effective at filtering out small-scale intra-grain noise, whilst retaining the edges of interest.

Edge detection resulted in a segmented binary image. Where radiometric and topographic imagery was being combined (Figure 1B), it was necessary to combine the two images, and this was done using a Boolean OR operator. The segmented binary images then needed to be segmented into non-intersecting regions which correspond to the structural units in the scene (Pal and Pal, 1993), in this case individual stones. The approach adopted here was based upon watershed segmentation, which is designed to separate just touching features (i.e. where no edge information is necessarily available) using a Euclidean Distance Map (EDM). The EDM assigns each pixel a value which is proportional to its distance from the nearest edge. These values produce peaks and troughs, with troughs along existing edges and peaks in the middle of stones. Where two edges are disconnected in an edge map, it is common for a trough to form along and between those edges. Hence, these troughs produce boundaries between touching features, where no edges were previously identified. The result is a set of closed edges, with the areas within them closely defining the features or stones that are of interest.

Finally, once the features produced using watershed segmentation have been labelled, it is necessary to extract grain-size information. As with other techniques, this should be done automatically. This was achieved by fitting and measuring an ellipse for each feature, which was assumed to correspond to the photograph a -axis. Determination of the b -axis has two options: (i) use of the minimum dimension revealed by the orthogonal to the a -axis; or (ii) determination of the value of b as that for which the ellipse

has the same area as the actual stone. The latter was adopted for this research. The software that is necessary for the ellipse-fitting is freely available via the internet.

3.3 Methodological testing

Methodological testing needed to consider both: (i) the effects of the various decisions reached during development of the image processing technique; and (ii) the extent to which rectified imagery and a high resolution DEM were needed to assist in the process. Thus, the following data sources were identified to assist with methodological testing:

- (a) as shown in Figure 1D, the edges of stones were manually traced by a cartographer from an orthoimage, and subject to the same data extraction process as the methods in Figures 1A to 1C, to provide an evaluation of the automated identification of individual stones, including the effects of thresholding;
- (b) the a - and b - axes of a random sample of 25 stones were measured using a rule on the manually-traced orthoimage and compared with the ellipse-based estimates of a - and b -axes from the same orthoimage, to test the grain-size extraction stage of the procedure;
- (c) a random sample of 25 stones from one image was identified and sampled from the flume experiment for which the photography was generated, and their a - and b - axes were measured, to test the extent to which a - and b - axes derived automatically from photography correspond to actual a - and b -axes; and
- (d) automatically-derived grain-size parameters (e.g. median grain-size) were compared with estimates obtained using conventional sieving of the surface particle layer, to provide a comparison that was dimensionally-consistent.

4. Results

4.1 Illustration of image processing stages

To illustrate the full range of image processing stages, Figure 2 shows the series of images produced for the method described in Figure 1B, as applied to the field data set. Figure 2c shows the effects of the basic thresholding of the orthophotograph (Figure 2a): it produces a reasonable discrimination between stones and background pixels and, in qualitative terms, comparison with the more sophisticated thresholding methods (e.g. entropy maximisation) suggested that this simple approach was best. The thresholded binary image was then cleaned using a simple closing algorithm (e.g. Russ, 1995) to remove interior holes which can lead to image over-segmentation at a later stage.

Figure 2d shows the effects of application of the edge detection algorithm to the DEM prior to thresholding and skeletonisation (Figure 2b). Use of the Hurst texture profiler allowed detection of pronounced cliffs in the surface where values of H were reduced. In particular, it was possible to reduce intra-grain noise in the H image, prior to thresholding and skeletonisation (see Figure 1b) by excluding the lowest order lags from the determination of H .

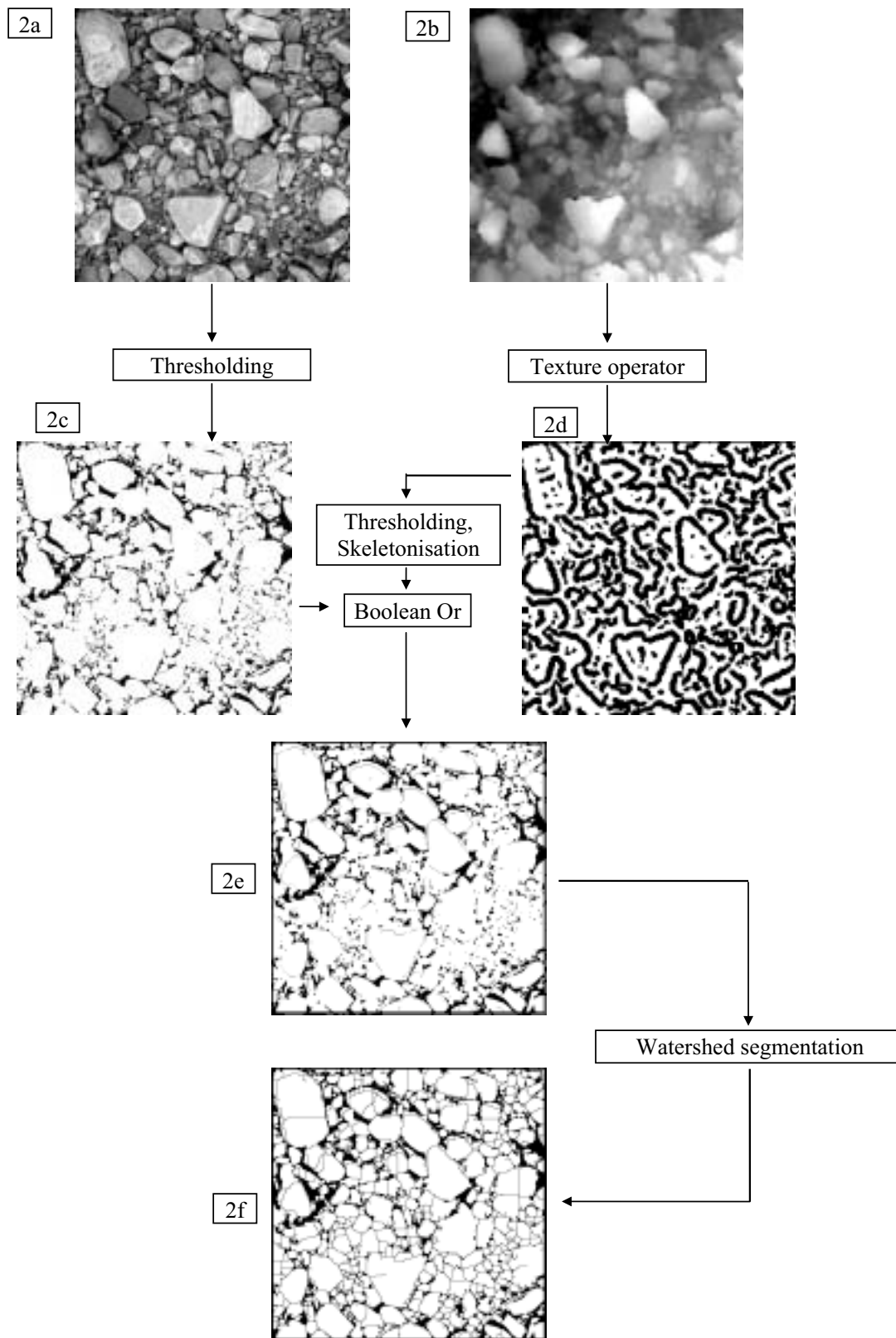


Fig. 2. Illustration of the steps used in image processing using Method 1B. 2a shows a rectified orthoimage and 2b a Digital Elevation Model. 2c shows the thresholded orthoimage and 2d the edges identified using the Hurst texture profiler. 2e shows the edge image after combination of 2c and 2d. 2f shows the edge image after watershed segmentation.

This ability to filter noise from an image is important, and one that can be adapted to suit the scale of the photography. Comparison of 2c and 2d emphasises why skeletonisation is necessary. Due to the nature of the stereomatching process, the resultant

DEM is about five times coarser than the associated orthophotograph, and hence the resolution of the Hurst texture image (2d) is poorer as compared with the edges associated with the thresholded image (2c). The edges introduced by skeletonisation of the

Hurst texture image (2d) can be seen in the finer lines on 2e. The next stage compared the thresholded orthophotograph with the edge detected image to produce 2e, illustrating one of the problems of using the DEM coupled to Hurst texture analysis: the associated Hurst edges in 2e are associated with the topographic edges of grains, rather than the actual edges apparent in 2a. This raises the question of what is a grain boundary, which has implications for whether or not DEM information needs to be used (see below). The final stage of the process uses watershed segmentation to grow edges until they connect (2f). In the example in Figure 2, the main edge growing is associated with the DEM-derived edges. Figure 2f suggests that this growing has resulted in significant over-segmentation, notably of the coarser grains. This is less of a problem if no DEM edge information is used (see below). Even then, such problems can only be assessed with reference to their effects upon the goals of the analysis: reliable estimates of particle size distribution. Thus, the effects of the automated edge detection algorithm represented in Figure 2 and Method 1B as a whole are compared with other automated edge detection methods (i.e. 1A and 1C) as well as manual edge detection methods (i.e. 1D).

4.2 Evaluation of the automated identification of stones

The first stage of the evaluation involves assessment of the ability of this method to identify individual stones, by comparing the results from Method 1A, with those obtained using Method 1D, for imagery obtained in both a field situation and a flume situation. Figure 3 shows cumulative frequency distributions comparing methods 1A and 1D, for both the field and the flume and selected quantitative results are summarised in Table 1. Figure 3 also shows the effects upon estimated frequency distributions of discounting grains estimated to have an a -axis less than 8mm in the flume case. This represents the lowest grain-size that Adams (1979) felt could be manually-estimated using photography of a scale similar to that used here, and the smallest grain-size that Wolman (1954) felt could be reliably sampled using grid-by-number methods.

In terms of the field data, the results are encouraging: there is a good level of correspondence in the cumulative frequency plots (Figure 3a, Table 1) for both manually and automatically derived distributions, and the methods identified a similar number of stones. Statistical testing of the grain-size statistics suggests that none are significantly different at the 95% level. However, the correspondence in the flume case is less encouraging. The frequency distributions including the 8mm particles are different (Table 1), and the methods identify a very different number of stones. However, if particles less than 8mm are excluded, there is a good level of agreement (Figure 3c) particularly for the coarser particles: there are no statistically-significant differences in estimates of mean a - or b - axis values; the number of particles identified is remarkably similar; and the median grain-size is estimated to at least about 20% of the smallest diameter (0.5 phi) used in conventional sieving (Table 1). The fact that in the flume case the two methods identified different numbers of stones, and that Method 1A produces grain-size statistics that are too coarse

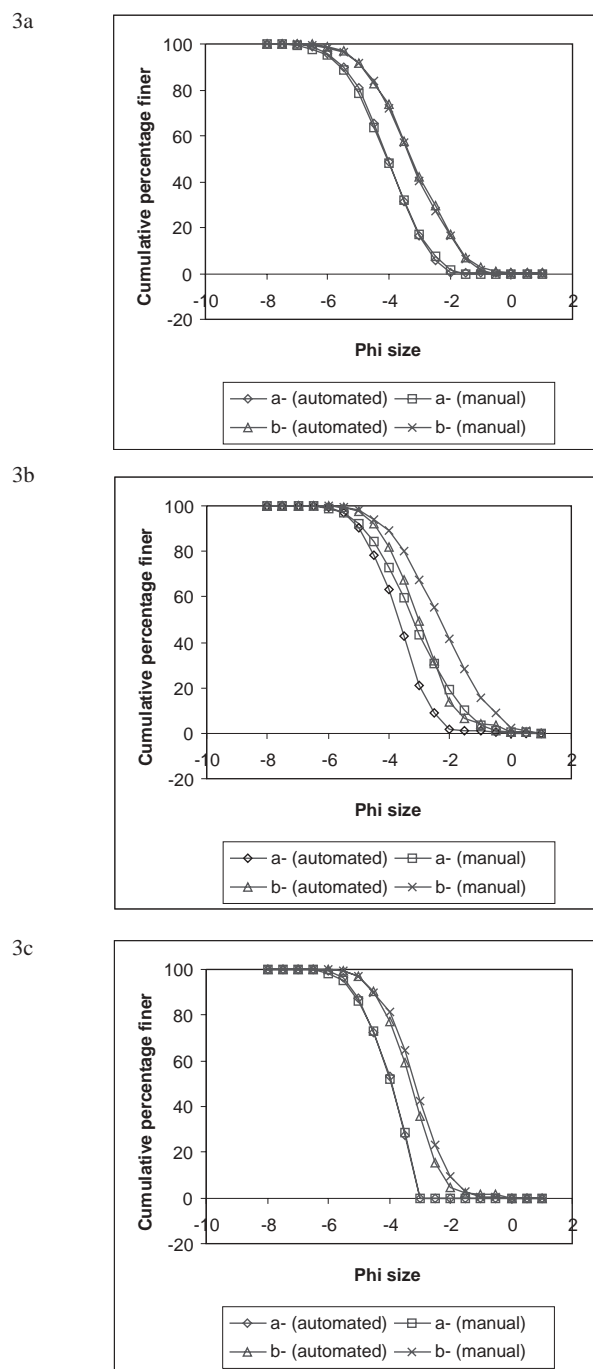


Fig. 3. Comparison of grainsize distributions obtained with automated (Method 1A) and manual (Method 1D) edge detection for the field case (3a), the flume case with all sizes (3b) and the flume case with a -axes greater than 8mm only (3c).

suggests that Method 1A is ineffective at identifying smaller grains in this case. Whilst exclusion of the finer than 8mm fraction may be justified by comparison with traditional Wolman (1954) sampling, it is important to note that this is ultimately determined by the scale of the imagery, and hence is associated with a trade-off between image scale and spatial coverage. It may be possible to estimate to fractions finer than 8mm by acquiring larger scale imagery. However, for a given camera format, this will reduce spatial coverage, so increasing the amount of analysis required to cover a given area.

Table 1. Comparison of grain-size statistics derived from automated edge extraction (Method 1A) as compared with manual edge extraction (Method 1D). All data are in phi units.

	<i>All sizes</i>				<i>Greater than 8mm only</i>			
	<i>a-</i>		<i>b-</i>		<i>a-</i>		<i>b-</i>	
<i>Method</i>	<i>1A</i>	<i>1D</i>	<i>1A</i>	<i>1D</i>	<i>1A</i>	<i>1D</i>	<i>1A</i>	<i>1D</i>
<i>Mean</i>	-3.71	-3.15	-3.00	-2.31	-4.06	-4.08	-3.32	-3.20
<i>Standard deviation</i>	0.95	1.31	1.08	1.35	0.72	0.76	0.93	0.94
<i>Median</i>	-3.68	-3.22	-3.00	-2.29	-3.92	-3.96	-3.29	-3.15
<i>Range</i>	6.34	8.36	6.64	7.59	3.60	3.63	5.90	5.37
<i>Count</i>	991	1347	991	1347	780	756	780	756
Field data	<i>All sizes</i>							
	<i>a-</i>		<i>b-</i>					
<i>Method</i>	<i>1A</i>	<i>1D</i>	<i>1A</i>	<i>1D</i>				
<i>Mean</i>	-4.10	-4.11	-3.26	-3.30				
<i>Standard deviation</i>	1.04	1.11	1.24	1.19				
<i>Median</i>	-4.02	-4.04	-3.23	-3.30				
<i>Range</i>	5.14	5.69	7.25	6.41				
<i>Count</i>	586	576	586	576				

4.3 Sensitivity to orthophotograph thresholding

Specific tests were undertaken to explore the sensitivity of grain-size estimates to selection of the thresholding parameter (T). This was undertaken by comparing estimates derived from Method 1A with those derived from 1D (Figure 4). These results suggested that median grain-size estimates did not vary significantly provided T was set at 100 or less. However, higher percentiles were more sensitive to T (Figure 4g). For instance, with $T=50$, higher estimates of D_{95} are obtained as compared with Method 1D, and this will result from too few edges due to under-segmentation. This allows identification of an optimal range of T values for D_{95} , with this imagery of $70 < T < 100$. For Figure 4, it becomes possible to identify the optimal threshold for this imagery, which was 70 in this case. This value of T , and the sensitivity of estimates to T values may vary between imagery, according to lighting conditions, image scale, image source and surface texture, such that further tests are required to establish its generality. However, this research shows how simple sensitivity testing with reference to a single manually-outlined image can identify an optimal thresholding value, which would apply to other imagery obtained from similar deposits, under similar lighting conditions, and at a similar scale.

4.4 Evaluation of ellipse-based measurement method

The second part of the method that needs to be evaluated is the ellipse-based particle measurement, by comparison with rule-estimates. Although this part of the method is common to 1A through 1D, this assessment used the manually-traced orthoimage (i.e. 1D), to avoid contamination by other competing factors (e.g. edge detection algorithm, orthorectification etc.). Figure 5 shows the comparison for both a - and b - axes for the flume data. The grains checked for this analysis were also those used for comparison with directly sampled and measured grains. For this, it was necessary to identify the same grain on an image as was measured on the image using a rule, and as was sampled from the surface manually. The flume data were used for this purpose as they gave greater control, and it was only possible to co-identify and co-register 25 of the coarser grains. This explains the coarser grain-size estimates shown in Table 2 and also means that the precision of the higher percentile estimates will be poor. Nevertheless, the level of correspondence between ellipse- and rule-estimates is encouraging (Table 2). The differences in the magnitude of the estimates of the coarsest particle sizes, those that would be expected to be most sensitive to this method, are very small. The mean grain-sizes are not significantly different at the 95% level.

Table 2. Statistics from comparing estimates of grain axes (a - and b -) directly measured with a rule from an orthoimage with those obtained using the automated ellipse placing, applied to Method 1D (manually-outlined grains). Flume data in phi units.

	<i>Ellipse-estimates</i> <i>a-</i>	<i>Rule-estimates</i> <i>a-</i>	<i>Ellipse-estimates</i> <i>b-</i>	<i>Rule-estimates</i> <i>b-</i>
<i>D50</i>	-5.89	-5.88	-5.19	-5.29
<i>D84</i>	-6.24	-6.22	-5.58	-5.68
<i>D95</i>	-6.43	-6.33	-5.82	-5.79

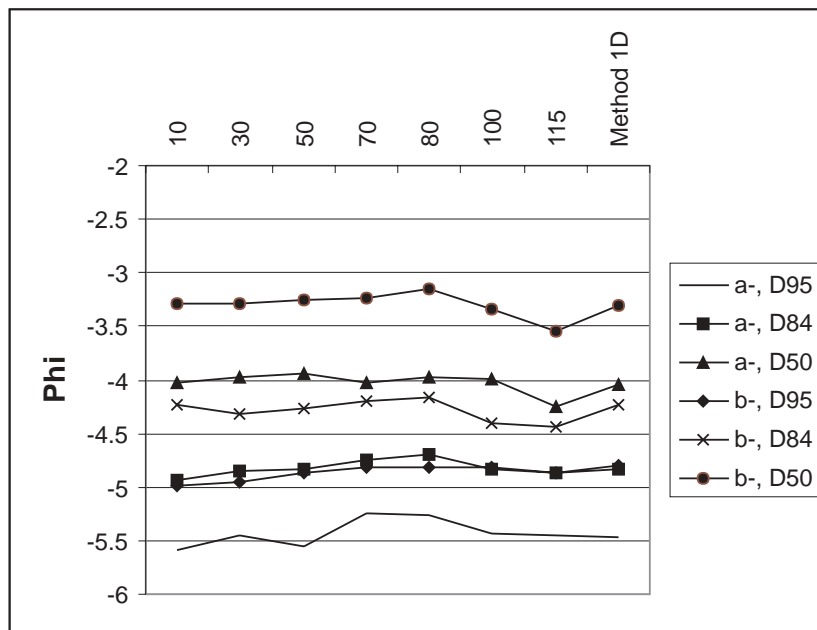
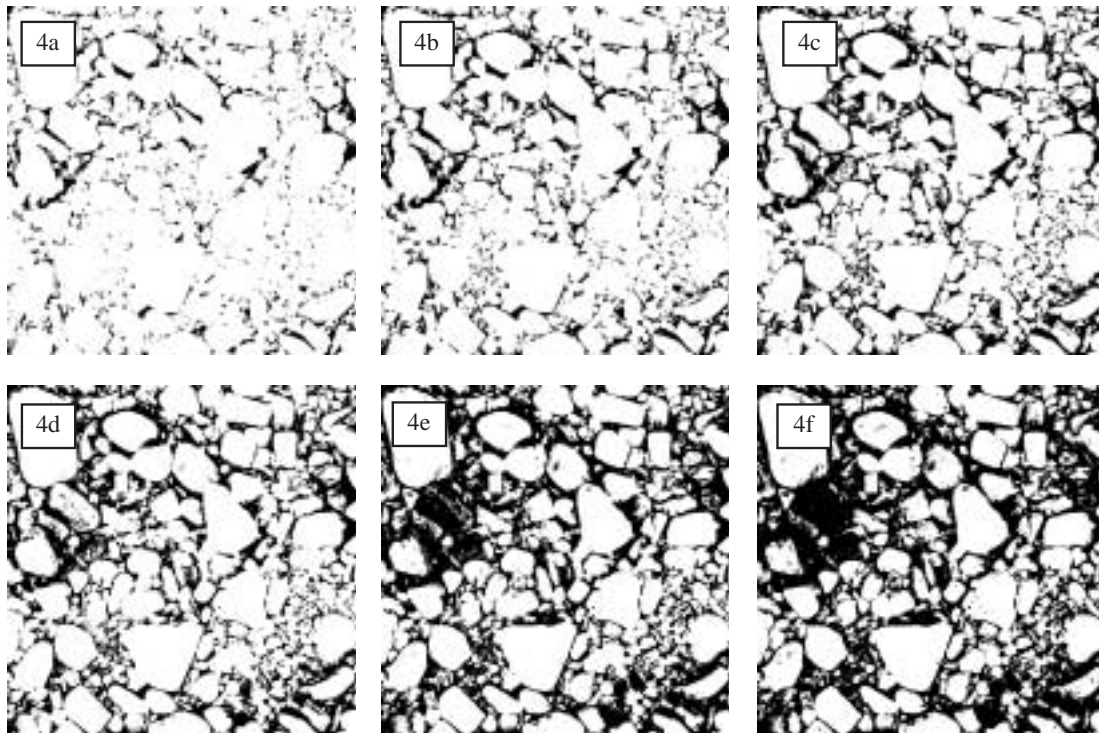


Fig. 4. The effects of different greyscale threshold values upon the orthoimage shown in Figure 2a: 4a = 30; 4b = 50; 4c = 70; 4d = 80; 4e = 100; 4f = 115; and 4g demonstrates the effects upon grain-size parameters.

Thus, the ellipse-based measurement method would seem appropriate for this type of analysis.

5. Assessment of different methods

The above sections have assessed the results of automated image analysis by comparing Method 1A, which involved the analysis of orthorectified imagery without the provision of additional DEM information, with Method 1D. This suggested (e.g. Figure 3) that the method could provide an excellent means of identifying the edges of particles as they appeared on the imagery and

quantifying their long and short axis dimensions. Two caveats were noted: the imagery needed to be of the right scale; and some attention has to be given to the initial thresholding of the image. Three important issues now need further discussion: (i) can these estimates be improved by the inclusion of additional edge information from a DEM?; (ii) is it necessary to use orthorectified imagery as opposed to raw imagery?; and (iii) how do these image-derived estimates of grain-size relate to those measured by traditional techniques such as Wolman (1954) grid-by-number sampling?

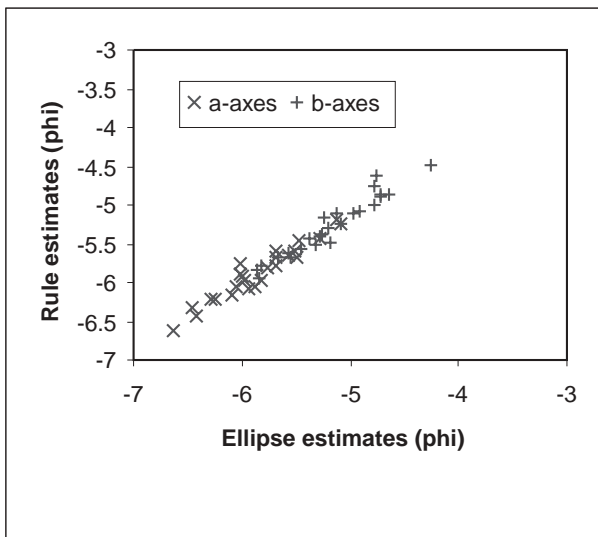


Fig. 5. Comparison of estimates of grain axes (a and b) directly measured with a rule from an orthoimage with those obtained using the automated ellipse placing applied to Method 1D (manually-outlined grains).

5.1 Assessment of the need for DEM information

First, inclusion of additional information derived from a DEM (Method 1B) did not result in a significant ($p=0.05$) improvement in estimates of mean b -axis values with respect to 1D. Comparison of Method 1B with 1A and 1D (Table 3) shows that all particle size estimates are less accurate when DEM information is added. This is perhaps surprising, but follows from patterns in Figure 2. First, the DEM information is necessarily downgraded in this study as the resolution provided by photogrammetrically-acquired DEMs is some multiple (typically about 5) of the original image or orthophotograph, due to the way that stereomatching algorithms operate during the digital photogrammetric process (*cf.* Figure 2d). Thus, the best grain resolution obtained from a DEM will not be as good as that which is obtained directly from an image. Thus, the DEM will not resolve particle boundaries to the same resolution as an image, and this was reflected in Figure 2e in terms of the difference in position of edges derived using the DEM as compared to those derived from the orthoimage. Second, with highly irregular grains, there is a high probability that topographic features are included that are not at the particle boundaries as seen on the image. Third, these two points exerted a significant effect upon the watershed segmentation process, encouraging over-segmentation. In combination, these three effects

explain why the percentiles identified using Method 1B are finer than those estimated using Method 1A (Table 3). These conclusions suggest that a DEM is not necessary, but it is also a reminder that image-based grain edges are not necessarily particle edges as defined using conventional measurement of a -, b - and c -axes. This is returned to briefly below. This is an important finding as high resolution DEMs are difficult to collect: access to sophisticated laser profiling devices may not be possible and techniques like digital photogrammetry are not straightforward at this scale (e.g. Butler *et al.*, 1998).

5.2 Assessment of the need for orthorectification

The above point that suggested that DEM information might not be necessary would be countered if orthorectified imagery were required, as this would also require a DEM, or at least a reasonably high density of ground control points. Comparison of Methods 1C and 1A (Table 3) suggested that use of raw imagery as opposed to orthorectified photography did not result in a statistically significant (at $p=0.05$) change in any of the derived grain-size parameters. Thus, this evidence suggests that it is possible to use raw, near-vertical imagery, without correction for image, tilt and relief distortion effects, provided the scale of that imagery is known.

5.3 Comparison of fully-automated particle size estimates with direct particle sampling measurements

The final stage of the assessment aimed to compare the estimates of grain-size characteristics obtained from the fully automated analysis (Method 1A) with those obtained from direct surface sampling of grains, using the dataset generated during assessment of the ellipse-based method (see above). As expected (e.g. Adams, 1979), there is a systematic bias present (Table 4, Figure 6), with automatically-measured b -axes systematically underestimated as compared with their actual sizes. The reasons for this are well-established. Analysis of the sort of 2D imagery shown in 2a does not recognise the three-dimensional structure of an individual particle, as well as the way in which particles are bedded together. Thus, the comparison of Methods 1A, 1B and 1C with 1D indicates which method is preferable for the identification of edges in two dimensions, as they appear in Figure 2a. This suggested that Methods 1A and 1C were preferable to Method 1B (Table 3), but this does not necessarily hold for analysis in three-dimensions, where Hurst texture profiling alone might be appro-

Table 3. Inter-comparison of different methods used to estimate grain-size characteristics for the field data. Method 1B data are provided after optimisation to include an amount of edge information that results in closest correspondence to Method 1D. All data are in phi units.

Threshold	a -			b -		
	$D95$	$D84$	$D50$	$D95$	$D84$	$D50$
Method 1A	-5.24	-4.74	-4.02	-4.82	-4.19	-3.23
Method 1B	-5.11	-4.63	-3.82	-4.56	-4.01	-3.00
Method 1C	-5.31	-4.76	-4.02	-4.81	-4.18	-3.12
Method 1D	-5.47	-4.84	-4.04	-4.80	-4.23	-3.30

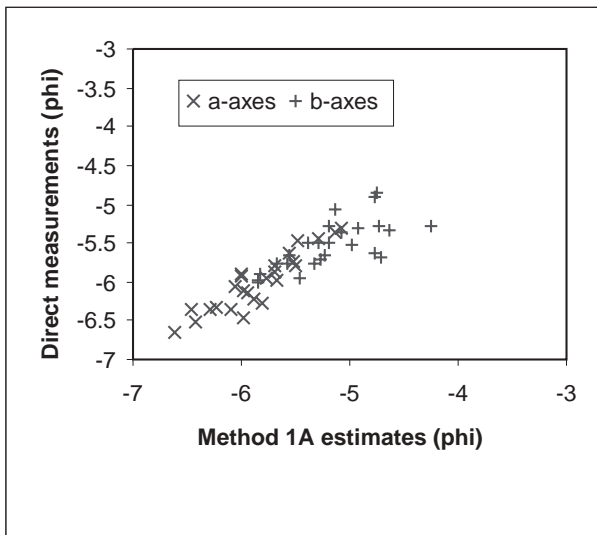


Fig. 6. Comparison of grain axes (*a* and *b*) measured by directly sampling stones from the surface with those estimated using the fully-automated method 1A.

appropriate. The main difficulty with using texture profiling alone, with the sort of complex gravel surfaces shown in Figure 2a, is that the edge information that is generated is highly skewed towards the coarser particle size distributions, with finer particles under-represented due to their much weaker topographic signal.

6. Conclusions

1. The results from this research are encouraging and suggest that it is possible to identify and quantify the edges of individual grains as they appear on unrectified digital imagery (scanned photographs or digital camera output), provided that it is of the correct scale with respect to the size of grains that are of interest. The methodology that is necessary to do this is described in Figure 1C, and sensitivity analysis is recommended to test the thresholding stage of the process, perhaps with reference to a single image that has been subject to manual edge delimitation.
2. Research is needed to assess whether or not this method can be extended to particles smaller than 8mm via an increase in image scale. Research is also needed to assess the extent to which ellipse-based methods may be used to estimate the third axis.
3. The grain-size estimates obtained automatically using this method are accurate with respect to manually-identified estimates, even though the technique is less effective at identifying the boundary of each grain exactly.

4. This paper does not seek to address the fundamental problem of any image-based analysis method, which relates to the correspondence between image-extracted parameters and traditional calliper-measured estimates. This is a problematic issue as any empirical relationship is likely to be spatially and temporally unstable due to spatial and temporal variation in the sedimentological structures formed by grain interactions (e.g. bedforms). However, it does provide a basic method for the rapid mapping of gravel sedimentologies over potentially large areas.
5. This research used relatively good imagery, obtained from exposed areas of gravel, with good lighting. Research is needed to assess the performance of the method in underwater areas, in areas where the imagery is of lower quality, and in areas where there are sand-gravel mixtures. The latter may be particularly problematic as even with large-scale imagery, sandy material may be mistaken as homogeneous and hence single, large, clasts. There is always the scope for manual editing in such situations.

Acknowledgements

JBB was in receipt of a NERC studentship and this research was also supported by NERC Grant GR9/3219 (awarded to SNL and Professor K.S. Richards) and EPSRC Grant GR/L58118 (awarded to SNL and JHC).

* Corresponding author

References

- ADAMS, J., 1979. Gravel size analysis from photographs. *American Society of Civil Engineers, ASCE Journal of the Hydraulics Division*, **104**, 1247-1255.
- ANDREWS, E.D., 1983. Entrainment of gravel from a naturally sorted riverbed material. *Bulletin of the Geological Society of America*, **94**, 1225-1231.
- BUFFINGTON, J.M., DIETRICH, W.E. and KIRCHNER, J.W., 1992. Friction angle measurements on a naturally formed gravel-bed: Implications for critical boundary shear stress. *Water Resources Research*, **28**, 411-25.
- BUTLER, J.B., 1999. High resolution photogrammetric monitoring and analysis of the structure of gravel-bed river surfaces. Thesis submitted in partial fulfilment of the requirements of the Ph.D. degree, University of Cambridge, 311pp.

Table 4. Statistics from comparing fully automated estimates of grain axes (*a*- and *b*-) with those directly measured by surface sampling. Flume data in phi units.

	Automated <i>a</i> -	Actual <i>a</i> -	Automated <i>b</i> -	Actual <i>b</i> -
<i>D</i> 50	-5.89	-5.97	-5.19	-5.52
<i>D</i> 84	-6.24	-6.35	-5.58	-5.76
<i>D</i> 95	-6.43	-6.47	-5.82	-5.95

- BUTLER, J.B., LANE, S.N. and CHANDLER, J.H., 1998. Assessment of DEM quality characterising surface roughness using close range digital photogrammetry. *Photogrammetric Record*, **16**, 271-91.
- CHURCH, M.A., 1970. *Baffin Island sandur. A study in Arctic fluvial environments*. Ph.D. thesis, University of British Columbia.
- CHURCH, M.A., McLEAN, D.G. and WOLCOTT, J.F., 1987b. River bed gravels : sampling and analysis. In Thorne, C.R., Bathurst, J.C. and Hey, R.D. (eds) *Sediment transport in gravel bed rivers*, Wiley, Chichester, 43-79, 1987.
- DAVIS, L.S., 1975. A survey of edge detection techniques. *Computer Graphics and Image Processing*, **4**, 248-70.
- DIEPENBROEK, M., BARTHOLOMA, A. and IBBEKEN, H., 1992. How round is round? A new approach to the topic of roundness by Fourier grain shape analysis. *Sedimentology*, **39**, 411-22.
- FAHNESTOCK, R.D., 1963. Morphology and hydrology of a glacial stream - White River, Mt. Rainier, Washington. *USGS Professional Paper*, **422-A**.
- FERGUSON, R.I. and PAOLA, C., 1997. Bias and precision of percentiles of bulk grain size distributions. *Earth Surface Processes and Landforms*, **22**, 1061-77.
- FU, K.S. and MUI, J.K., 1981. A survey on image segmentation. *Pattern Recognition*, **13**, 3-16.
- GOMEZ, B., 1979. A technique for sampling the surface bed material in mixed sand and gravel-bed streams. *BGRG Technical Bulletin*, **24**, 15-23.
- HARALICK, R.M. and SHAPIRO, L.G., 1985. Image segmentation techniques. *Computer Vision Graphics and Image Processing*, **29**, 100-32.
- HEY, R.D. and THORNE, C.R., 1983. Accuracy of surface samples from gravel-bed material. *ASCE Journal of the Hydraulics Division*, **109**, 842-851.
- HURST, H.E., BLACK, R.P. and SIMAIKA, Y.M., 1965. *Long-term storage: an experimental study*, Constable, London.
- IRIONDO, M.H., 1972. A rapid method for size analysis of coarse sediments. *Journal of Sedimentary Petrology*, **42**, 985-986.
- KAPUR, J.N., SAHOO, P.K. and WONG, A.K.C., 1985. A new method for grey-level picture thresholding using the entropy of the histogram. *Computer Vision Graphics and Image Processing*, **29**, 100-32.
- KELLERHALS, R., 1967. Stable channels with gravel-paved beds. *ASCE Journal of the Hydraulics Division*, **93**, 63-84.
- KELLERHALS, R. and BRAY, D.I., 1971. Sampling procedure for fluvial sediments. *ASCE Journal of the Hydraulics Division*, **97**, 1165-1180.
- KELLERHALS, R., 1967. Stable channels with gravel-paved beds. *ASCE Journal of the Hydraulics Division*, **93**, 63-84.
- KELLERHALS, R. and BRAY, D.I., 1971. Sampling procedure for fluvial sediments. *ASCE Journal of the Hydraulics Division*, **97**, 1165-1180.
- KIRCHNER, J.W., DIETRICH, W.E., ISEYA, F. and IKEDA, H., 1990. The variability of critical shear stress, friction angle and grain protrusion in water-worked sediments. *Sedimentology*, **37**, 647-72.
- KLINGEMANN, P.C. and EMMETT, W.W., 1982. Gravel bedload transport processes. In Hey, R.D., Bathurst, J.C. and Thorne, C.R. (eds), *Gravel-Bed Rivers*, Wiley, Chichester, 141-169.
- KOHLER, R., 1981. A segmentation system based on thresholding. *Computer Graphics and Image Processing*, **15**, 319-38.
- KOMAR, P.D. and LI, Z., 1988. Applications of grain-pivoting and sliding analysis to selective entrainment of gravel and to flow-competence evaluations. *Sedimentology*, **35**, 681-695.
- LANE, S.N., PORFIRI, K. and CHANDLER, J.H., in press. Monitoring flume channel surfaces using close range photogrammetry. Forthcoming in *ASCE Journal of Hydraulic Engineering*.
- McEWAN, I. K., SHEEN, T., CUNNINGHAM, G. J. and ALLEN, A. R., 2000. Estimating the size composition of sediment surfaces through image analysis. Forthcoming in *Proceedings of the Institute of Civil Engineers: Water, Maritime & Energy*.
- MOSLEY, M.P. and TINDALE, D.S., 1985. Sediment variability and bed material sampling in gravel-bed rivers. *Earth Surface Processes and Landforms*, **10**, 465-482.
- PAL, N.R. and PAL, S.K., 1993. A review of image segmentation techniques. *Pattern Recognition*, **26**, 1277-94.
- PARKER, G., DHAMOTHARAN, S. and STEFAN, H., 1982. Model experiments on mobile, paved, gravel-bed streams. *Water Resources Research*, **18**, 1395-1408.
- PICKUP, G., 1981. A bed material sampler for use in coarse gravels and armoured beds. *BGRG Technical Bulletin*, **29**, 33-38.
- RICE, S. and CHURCH, M., 1996. Sampling surficial fluvial gravels: The precision of size distribution percentile estimates. *Journal of Sedimentary Research*, **66**, 654-65.
- RUSS, J.C., 1994. *Fractal Surfaces*, Plenum Press, New York.
- RUSS, J.C., 1995. *The Image Processing Handbook*, CRC Press, Boca Baton.
- SHIELDS, A., 1936. Anwendung der aehnlichkeitsmechanik und der turbulenz-forschung auf die geschiebebewegung. *Mitteilung der Preussischen Fersuchsanstalt fuer Wasserbau und Schiffbau*, Heft **26**, Berlin.
- STRICKLER, A., 1923. Beitrage zur Frage der Geschwindigkeitsformel und der Rauhigkeitszahlen fur Strome, Kanale und Geschlossene Leitungen. *Mitteilungen des Eidgenossischer Amtes fur Wasserwirtschaft*, Bern, Switzerland, 16g.
- TAXT, T., FLYNN, P.J. and JAIN, A.K., 1989. Segmentation of document images. *IEEE Transactions on Pattern Analysis and Machine Intelligence*, **11**, 1322-9.
- WOLF, P.R., 1983. *Elements of Photogrammetry*. McGraw Hill, London, 663pp.
- WOLMAN, M.G., 1954. A method of sampling coarse river bed material. *Transactions of the American Geophysical Union*, **35**, 951-956.